

Original citation:

Wei, Xiaojun and Živanović, Stana (2018) Frequency response function-based explicit framework for dynamic identification in human-structure systems. *Journal of Sound and Vibration*, 422 . pp. 453-470. doi:10.1016/j.jsv.2018.02.015

Permanent WRAP URL:

<http://wrap.warwick.ac.uk/100474>

Copyright and reuse:

The Warwick Research Archive Portal (WRAP) makes this work by researchers of the University of Warwick available open access under the following conditions. Copyright © and all moral rights to the version of the paper presented here belong to the individual author(s) and/or other copyright owners. To the extent reasonable and practicable the material made available in WRAP has been checked for eligibility before being made available.

Copies of full items can be used for personal research or study, educational, or not-for-profit purposes without prior permission or charge. Provided that the authors, title and full bibliographic details are credited, a hyperlink and/or URL is given for the original metadata page and the content is not changed in any way.

Publisher's statement:

© 2018, Elsevier. Licensed under the Creative Commons Attribution-NonCommercial-NoDerivatives 4.0 International <http://creativecommons.org/licenses/by-nc-nd/4.0/>

A note on versions:

The version presented here may differ from the published version or, version of record, if you wish to cite this item you are advised to consult the publisher's version. Please see the 'permanent WRAP url' above for details on accessing the published version and note that access may require a subscription.

For more information, please contact the WRAP Team at: wrap@warwick.ac.uk

1 **Frequency response function-based explicit framework for dynamic**
2 **identification in human-structure systems**

3

4

Xiaojun Wei*, Stana Živanović

5

School of Engineering, University of Warwick, CV4 7AL, UK

6

*Corresponding author

7

E-mail address: x.wei.3@warwick.ac.uk; S.Zivanovic@warwick.ac.uk

8

9

Abstract

10 The aim of this paper is to propose a novel theoretical framework for dynamic identification
11 in a structure occupied by a single human. The framework enables the prediction of the
12 dynamics of the human-structure system from the known properties of the individual system
13 components, the identification of human body dynamics from the known dynamics of the
14 empty structure and the human-structure system and the identification of the properties of the
15 structure from the known dynamics of the human and the human-structure system. The
16 novelty of the proposed framework is the provision of closed-form solutions in terms of
17 frequency response functions obtained by curve fitting measured data. The advantages of the
18 framework over existing methods are that there is neither need for nonlinear optimisation nor
19 need for spatial/modal models of the empty structure and the human-structure system. In
20 addition, the second-order perturbation method is employed to quantify the effect of
21 uncertainties in human body dynamics on the dynamic identification of the empty structure
22 and the human-structure system. The explicit formulation makes the method computationally
23 efficient and straightforward to use. A series of numerical examples and experiments are
24 provided to illustrate the working of the method.

25 **Keywords:** Human-structure interaction; system identification; human body dynamics;
26 explicit framework; frequency response function.

27 **1. Introduction**

28 Dynamic interaction between a human and a low-frequency structure supporting the human is
29 a well-recognised phenomenon that has become increasingly prominent over the last two
30 decades due to the increase in slenderness of modern structures [1-4]. Naturally, the dynamic
31 properties of the human-structure system are influenced by the interplay of dynamics of the
32 two subsystems and they differ from those of the structure itself [1-7]. When considering the
33 vertical flexural vibration modes of a structure, the human occupancy is known to cause a
34 shift in the natural frequency and an increase in the damping ratio [3, 8-10]. Knowledge of
35 the dynamic properties of both the occupant(s) and the structure is crucial for developing
36 better understanding of the extent of the human-structure interaction and its influence on the
37 dynamic response analysis and vibration control design for structures accommodating
38 humans.

39 In structural engineering applications, the dynamics of a human are usually described using a
40 single-degree-of-freedom (SDOF) mass-spring-damper model [3, 6, 9-14]. The dynamics of a
41 structure are often described utilising a spatial model or a modal model (having, say, n DOFs)
42 that can be established using either finite element method or modal analysis [15]. The human-
43 structure system can then be represented by a $n + 1$ DOFs model whose modal properties are
44 determined from an eigenvalue analysis, either numerically or analytically [9, 15, 16].

45 Key challenge in studying human-structure systems is the identification of the properties of
46 the human model. Several approaches have been proposed for this purpose. For example,
47 Griffin and his colleagues [17, 18] estimated the dynamic properties of a human in a standing

48 or sitting posture by curve fitting measured driving-point apparent masses. On the other hand,
49 Foschi et al. [19] estimated the frequency and damping ratio of a human in a standing posture
50 by minimising differences between the computed and measured displacement responses of
51 the human-floor system exposed to a heel-drop impact. Zheng and Brownjohn [6] measured
52 frequency response functions (FRFs) of both the empty structure and the human-structure
53 system. After identifying a SDOF modal model for a vibration mode of interest from the
54 measured FRFs of the empty structure, they combined this model with assumed properties of
55 the human to derive the eigenvalues of the human-structure system. They used a nonlinear
56 optimisation method to identify the properties of the human that result in the best match
57 between the eigenvalues of the human-structure system and the measured counterparts. This
58 procedure was also employed by Shahabpoor et al. [13] to identify a SDOF model for a
59 walking human. Sachse [2] used a similar procedure for identifying the human's dynamic
60 properties, the only difference being that she compared the measured and calculated FRFs of
61 the human-structure system rather than the eigenvalues. This method was also used by Van
62 Nimmen et al. [14] to identify a SDOF model for a stationary crowd. Jones et al. [20]
63 summarised the dynamic properties of the human in a standing posture reported in the
64 literature. The properties vary significantly between individuals: natural frequency was in the
65 range from 3.3 Hz to 10.4 Hz while damping ratio was between 33% and 69%. Human body
66 dynamics are also found to vary with postures [14, 18, 21].

67 Most research is devoted to identifying the dynamics of the human body and predicting the
68 dynamics of human-structure systems. These studies were performed with a sole purpose in
69 mind: to develop dynamic models of humans, either standing or sitting, and then to add them
70 to the dynamic model of an empty structure, usually a grandstand, to predict the dynamic
71 response of the human-structure system in sports or music events [10, 20, 22]. Little attention
72 has been paid to identifying the dynamics of the empty structure provided the dynamics of

73 the human-structure system are known. This scenario is relevant in manually operated impact
74 hammer modal testing in which a hammer operator is present on the structure during data
75 collection. The identification of dynamic properties of the structure routinely neglects the
76 presence of the hammer operator and it assumes that the dynamics of the empty structure are
77 the same as those of the hammer operator-structure system. This assumption might be
78 erroneous since the interaction between a single human and a structure is important in some
79 cases, such as for ultra-lightweight fibre reinforced polymer (FRP) footbridges. Although
80 some existing methods for identifying human body dynamics [2, 6, 13, 14] can also be used,
81 at least in some cases, for the dynamic identification of the empty structure, they are not
82 necessarily convenient to apply.

83 To the best knowledge of the authors, there does not exist a single theoretical framework
84 which offers both closed-form solutions and flexibility of being used for any of the three
85 applications as and when needed, i.e. the prediction of the dynamics of the human-structure
86 system when the dynamics of individual systems are known, the identification of human body
87 dynamics when the empty structure and human-structure system dynamics are known and the
88 identification of the empty structure when the human and human-structure dynamics are
89 known. This paper proposes a unifying and simple to implement framework for determining
90 the dynamics of any one of the three systems in terms of the dynamics of the other two. The
91 framework provides closed-form solutions for identifying the dynamics of the system under
92 study and therefore does not require utilisation of nonlinear optimisation techniques inherent
93 to some other studies [2, 6, 13, 14]. The framework utilises curve-fitted FRFs (i.e.
94 receptances, mobilities or accelerances) directly as opposed to using FRFs to derive spatial or
95 modal models of the empty structure and the human-structure system required in some other
96 studies [2, 6, 13, 14]. In addition, the second-order perturbation method is utilised to quantify
97 the effect of uncertainties in human body dynamics on the dynamic identification of the

98 empty structure and the human-structure system. The paper focuses on low-frequency
99 structures (i.e. vibration modes with natural frequencies up to about 8Hz) on which the
100 human-structure interaction is expected to be strongest. In this frequency region, the human is
101 modelled as a SDOF system since only their first vibration mode is likely to interact with the
102 structure. The proposed method is applicable for problems involving humans in any
103 stationary posture (e.g. standing, sitting and crouching to perform the impact hammer test).
104 Future work will be dedicated to generalise the framework for the crowd-structure interaction.

105 Following this introductory section, Section 2 introduces the novel method in the context of
106 identifying properties of a human-structure system. Use of the proposed method for
107 identifying human body dynamics is presented in Section 3, whilst its use for estimating
108 dynamics of the empty structure is presented in Section 4. Each section is supported by
109 numerical examples and/or experiments. Conclusions are drawn in Section 5.

110 **2. Identification of the dynamics of a human-structure system**

111 This section presents the theoretical framework followed by a numerical example. The
112 proposed framework was inspired by the studies in the research fields of vibration control
113 [23-25] and nonlinear dynamics [26].

114 **2.1. Theoretical framework**

115 The equation of forced vibration of a linear structure having n DOFs may be cast in second
116 order form as

$$117 \quad \mathbf{M}_s \ddot{\mathbf{x}}_s + \mathbf{C}_s \dot{\mathbf{x}}_s + \mathbf{K}_s \mathbf{x}_s = \mathbf{f}_s \quad (1)$$

118 where

$$119 \quad \mathbf{M}_s = \begin{bmatrix} m_{11}^s & L & m_{1(n-1)}^s & m_{1n}^s \\ M & O & M & M \\ m_{(n-1)1}^s & L & m_{(n-1)(n-1)}^s & m_{(n-1)n}^s \\ m_{n1}^s & L & m_{n(n-1)}^s & m_{nn}^s \end{bmatrix}, \mathbf{C}_s = \begin{bmatrix} c_{11}^s & L & c_{1(n-1)}^s & c_{1n}^s \\ M & O & M & M \\ c_{(n-1)1}^s & L & c_{(n-1)(n-1)}^s & c_{(n-1)n}^s \\ c_{n1}^s & L & c_{n(n-1)}^s & c_{nn}^s \end{bmatrix},$$

$$120 \quad \mathbf{K}_s = \begin{bmatrix} k_{11}^s & L & k_{1(n-1)}^s & k_{1n}^s \\ M & O & M & M \\ k_{(n-1)1}^s & L & k_{(n-1)(n-1)}^s & k_{(n-1)n}^s \\ k_{n1}^s & L & k_{n(n-1)}^s & k_{nn}^s \end{bmatrix}, \mathbf{x}_s = \begin{bmatrix} x_1^s \\ M \\ x_{n-1}^s \\ x_n^s \end{bmatrix}, \mathbf{f}_s = \begin{bmatrix} f_1^s \\ M \\ f_{n-1}^s \\ f_n^s \end{bmatrix}.$$

121 \mathbf{M}_s , \mathbf{C}_s and $\mathbf{K}_s \in R^{n \times n}$ are the mass, damping and stiffness matrices. \mathbf{f}_s , \mathbf{x}_s , $\dot{\mathbf{x}}_s$, $\ddot{\mathbf{x}}_s \in R^{n \times 1}$ are
 122 the external force, displacement, velocity and acceleration vectors, respectively. R denotes
 123 the field of real numbers. Dot denotes the derivative with respect to time.

124 Eq. (1) may be written in Laplace domain as

$$125 \quad \mathbf{Z}_s(s) \mathbf{X}_s(s) = \mathbf{F}_s(s) \quad (2)$$

126 where $\mathbf{Z}_s(s) = (\mathbf{M}_s s^2 + \mathbf{C}_s s + \mathbf{K}_s)$, s is the Laplace variable, whilst $\mathbf{X}_s(s)$ and $\mathbf{F}_s(s)$ are the
 127 Laplace transforms of displacement and force vectors.

128 When a stationary human occupies a structure, the structure and the human form a new joint
 129 system whose dynamics are influenced by the dynamics of the two individual components. In
 130 line with the previous research, the human is modelled as a SDOF system having mass m_h ,
 131 damping c_h and stiffness k_h . m_h is assumed to represent the full mass of the human, as
 132 implemented in some previous studies [11, 19, 27-30]. Without loss of generality, it is

133 assumed that the human is located at the n -th degree of freedom of the structure. Therefore,
 134 the forced-vibration of the human-structure system can be described by

$$135 \quad \mathbf{M}_{sh} \ddot{\mathbf{x}}_{sh} + \mathbf{C}_{sh} \dot{\mathbf{x}}_{sh} + \mathbf{K}_{sh} \mathbf{x}_{sh} = \mathbf{f}_{sh} \quad (3)$$

136 where

$$137 \quad \mathbf{M}_{sh} = \begin{bmatrix} m_{11}^s & L & m_{1(n-1)}^s & m_{1n}^s & 0 \\ M & O & M & M & M \\ m_{(n-1)1}^s & L & m_{(n-1)(n-1)}^s & m_{(n-1)n}^s & 0 \\ m_{n1}^s & L & m_{n(n-1)}^s & m_{nn}^s & 0 \\ 0 & L & 0 & 0 & m_h \end{bmatrix}, \quad \mathbf{C}_{sh} = \begin{bmatrix} c_{11}^s & L & c_{1(n-1)}^s & c_{1n}^s & 0 \\ M & O & M & M & M \\ c_{(n-1)1}^s & L & c_{(n-1)(n-1)}^s & c_{(n-1)n}^s & 0 \\ c_{n1}^s & L & c_{n(n-1)}^s & c_{nn}^s + c_h & -c_h \\ 0 & L & 0 & -c_h & c_h \end{bmatrix},$$

$$138 \quad \mathbf{K}_{sh} = \begin{bmatrix} k_{11}^s & L & k_{1(n-1)}^s & k_{1n}^s & 0 \\ M & O & M & M & M \\ k_{(n-1)1}^s & L & k_{(n-1)(n-1)}^s & k_{(n-1)n}^s & 0 \\ k_{n1}^s & L & k_{n(n-1)}^s & k_{nn}^s + k_h & -k_h \\ 0 & L & 0 & -k_h & k_h \end{bmatrix}, \quad \mathbf{x}_{sh} = \begin{bmatrix} x_1^s \\ x_{n-1}^s \\ x_n^s \\ x_h \end{bmatrix}, \quad \mathbf{f}_{sh} = \begin{bmatrix} f_1^s \\ M \\ f_{n-1}^s \\ f_n^s \\ 0 \end{bmatrix}.$$

139 Eq. (3) may be expressed in Laplace domain as

$$140 \quad \mathbf{Z}_{sh}(s) \mathbf{X}_{sh}(s) = \mathbf{F}_{sh}(s) \quad (4)$$

141 where

$$\begin{aligned}
 \mathbf{Z}_{sh}(s) &= (\mathbf{M}_{sh}s^2 + \mathbf{C}_{sh}s + \mathbf{K}_{sh}) \\
 &= \begin{bmatrix} \mathbf{Z}_s(s)_{n \times n} & \mathbf{0}_{n \times 1} \\ \mathbf{0}_{1 \times n} & m_h s^2 \end{bmatrix} + \begin{bmatrix} \mathbf{0}_{(n-1) \times (n-1)} & \mathbf{0}_{(n-1) \times 1} & \mathbf{0}_{(n-1) \times 1} \\ \mathbf{0}_{1 \times (n-1)} & (c_h s + k_h) & -(c_h s + k_h) \\ \mathbf{0}_{1 \times (n-1)} & -(c_h s + k_h) & (c_h s + k_h) \end{bmatrix} \\
 &= \begin{bmatrix} \mathbf{Z}_s(s)_{n \times n} & \mathbf{0}_{n \times 1} \\ \mathbf{0}_{1 \times n} & m_h s^2 \end{bmatrix} + \mathbf{u}(s) \mathbf{u}^T(s) \\
 &= \mathbf{Z}_{sm}(s) + \mathbf{u}(s) \mathbf{u}^T(s).
 \end{aligned}$$

142

143 In this expression, $\mathbf{u}(s) = \begin{bmatrix} 64 \sqrt{7-148} & 0 & \sqrt{c_h s + k_h} & -\sqrt{c_h s + k_h} \end{bmatrix}^T$, $(\bullet)^T$ is the transpose of (\bullet) .

144 For the sake of clarity, dimensions of some matrices are stated in the equation.

145 The receptance matrix of the human-structure system is

$$146 \quad \mathbf{H}_{sh}(s) = (\mathbf{Z}_{sh}(s))^{-1} = (\mathbf{Z}_{sm}(s) + \mathbf{u}(s) \mathbf{u}^T(s))^{-1}. \quad (5)$$

147 Let us denote

$$148 \quad \mathbf{H}_{sm}(s) = \mathbf{Z}_{sm}^{-1}(s) = \begin{bmatrix} \mathbf{H}_s(s) & \mathbf{0}_{n \times 1} \\ \mathbf{0}_{1 \times n} & \frac{1}{m_h s^2} \end{bmatrix} \quad (6)$$

149 where $\mathbf{H}_s(s) = \mathbf{Z}_s^{-1}(s)$ is the receptance matrix of the empty structure.

150 According to the Sherman-Morrison formula [31], the receptance matrix of the human-
151 structure system can be re-written as

$$152 \quad \mathbf{H}_{sh}(s) = \mathbf{H}_{sm}(s) - \frac{\mathbf{H}_{sm}(s) \mathbf{u}(s) \mathbf{u}^T(s) \mathbf{H}_{sm}(s)}{1 + \mathbf{u}^T(s) \mathbf{H}_{sm}(s) \mathbf{u}(s)}. \quad (7)$$

153 Therefore, the receptance matrix of the human-structure system can be obtained using the
 154 receptance matrix of the empty structure and the mass, damping and stiffness properties of
 155 the human.

156 The pn -th ($p \leq n$) receptance of the human-structure system may be obtained by pre-
 157 multiplying and post-multiplying Eq. (7) by \mathbf{e}_p^T and \mathbf{e}_n , respectively,

$$158 \quad h_{pn}^{sh}(s) = \mathbf{e}_p^T \mathbf{H}_{sm}(s) \mathbf{e}_n - \frac{\mathbf{e}_p^T \mathbf{H}_{sm}(s) \mathbf{u}(s) \mathbf{u}^T(s) \mathbf{H}_{sm}(s) \mathbf{e}_n}{1 + \mathbf{u}^T(s) \mathbf{H}_{sm}(s) \mathbf{u}(s)} \quad (8)$$

159 where \mathbf{e}_i^T is a vector of dimension $(n+1) \times 1$, whose i -th entry is unity and the other entries are
 160 zero.

161 Due to

$$162 \quad \mathbf{e}_p^T \mathbf{H}_{sm}(s) \mathbf{e}_n = h_{pn}^s(s) \quad (9)$$

$$163 \quad \mathbf{e}_p^T \mathbf{H}_{sm}(s) \mathbf{u}(s) = \sqrt{c_h s + k_h} h_{pn}^s(s) \quad (10)$$

$$164 \quad \mathbf{u}^T(s) \mathbf{H}_{sm}(s) \mathbf{e}_n = \sqrt{c_h s + k_h} h_{nn}^s(s) \quad (11)$$

165 and

$$166 \quad \mathbf{u}^T(s) \mathbf{H}_{sm}(s) \mathbf{u}(s) = (c_h s + k_h) \left(h_{nn}^s(s) + \frac{1}{m_h s^2} \right) \quad (12)$$

167 where $h_{nn}^s(s)$ is the direct receptance at the n -th DOF and $h_{pn}^s(s)$ is the cross receptance
 168 between the p -th output and the n -th input, both related to the empty structure, Eq. (8) now
 169 becomes

$$170 \quad h_{pn}^{sh}(s) = h_{pn}^s(s) - \frac{(c_h s + k_h) h_{pn}^s(s) h_{nn}^s(s)}{1 + (c_h s + k_h) \left(h_{nn}^s(s) + \frac{1}{m_h s^2} \right)} \quad (13)$$

171 which indicates that the pn -th cross receptance of the human-structure system may be
 172 calculated using the $h_{nn}^s(s)$ and $h_{pn}^s(s)$ of the empty structure and the dynamic properties of
 173 the human.

174 If $p = n$, then

$$175 \quad h_{nn}^{sh}(s) = h_{nn}^s(s) - \frac{(c_h s + k_h) h_{nn}^s(s) h_{nn}^s(s)}{1 + (c_h s + k_h) \left(h_{nn}^s(s) + \frac{1}{m_h s^2} \right)} \quad (14)$$

176 which indicates that the direct receptance of the human-structure system could be calculated
 177 using $h_{nn}^s(s)$ of the empty structure and the dynamic properties of the human.

178 The denominator of Eqs. (13) or (14) generates the characteristic equation

$$179 \quad 1 + (c_h s + k_h) \left(h_{nn}^s(s) + \frac{1}{m_h s^2} \right) = 0 \quad (15)$$

180 from which the eigenvalues (and therefore natural frequencies and damping ratios) of the
 181 human-structure system can be calculated.

182 **2.2. Effect of uncertainties in human properties on predicting the dynamics of the**
183 **human-structure system**

184 The dynamic properties of the human body may vary due to small postural changes and/or
185 changes in vibration response level. These variations inevitably affect the dynamic prediction
186 of the human-structure system. The second-order perturbation method [32] could be used to
187 estimate the effect of the uncertainties. The perturbation method is based on the Taylor series
188 expansion of the system response around the mean value of the input parameters and it is
189 used to compute the expectations and moments of the output parameters.

190 Here, the small variations in the stiffness and damping of the human body are considered. No
191 variation in the mass is considered since the mass can be measured accurately. It is assumed
192 that the stiffness and damping of the human body are independent normal random variables.
193 The expectation and standard deviation of the stiffness are E_{k_h} and σ_{k_h} , respectively, while
194 for the damping these are E_{c_h} and σ_{c_h} .

195 The magnitude and phase of the pn -th receptance of the joint system may be expressed as

196
$$|h_{pn}^{sh}(s)| = \sqrt{\left(\operatorname{Re}(h_{pn}^{sh}(s))\right)^2 + \left(\operatorname{Im}(h_{pn}^{sh}(s))\right)^2} \quad (16)$$

197 and

198
$$\angle h_{pn}^{sh}(s) = \arctan\left(\frac{\operatorname{Im}(h_{pn}^{sh}(s))}{\operatorname{Re}(h_{pn}^{sh}(s))}\right) \quad (17)$$

199 where $|(g)|$ is the magnitude of (g) ; $\angle(g)$ is the phase of (g) ; and $\text{Re}(g)$ and $\text{Im}(g)$ are the
 200 real and imaginary parts of (g) . Eq. (13) infers that the magnitude and phase are functions of
 201 the damping and stiffness of the human body. The expectation and standard deviation of the
 202 magnitude can be expressed as Eqs. (18) and (19) using the second-order perturbation method
 203 [32].

$$204 \quad E(|h_{pn}^{sh}(s)|) \approx |h_{pn}^{sh}(s)|_{\substack{c_h=E_{c_h} \\ k_h=E_{k_h}}} + \frac{1}{2} \left(\frac{\partial^2 |h_{pn}^{sh}(s)|}{\partial c_h^2} \Big|_{\substack{c_h=E_{c_h} \\ k_h=E_{k_h}}} \sigma_{c_h}^2 + \frac{\partial^2 |h_{pn}^{sh}(s)|}{\partial k_h^2} \Big|_{\substack{c_h=E_{c_h} \\ k_h=E_{k_h}}} \sigma_{k_h}^2 \right) \quad (18)$$

205 and

$$206 \quad \sigma(|h_{pn}^{sh}(s)|) \approx \sqrt{\left(\frac{\partial |h_{pn}^{sh}(s)|}{\partial c_h} \Big|_{\substack{c_h=E_{c_h} \\ k_h=E_{k_h}}} \right)^2 \sigma_{c_h}^2 + \left(\frac{\partial |h_{pn}^{sh}(s)|}{\partial k_h} \Big|_{\substack{c_h=E_{c_h} \\ k_h=E_{k_h}}} \right)^2 \sigma_{k_h}^2} \quad (19)$$

207 where $E(g)$ is the expectation of (g) ; $\sigma(g)$ is the standard deviation of (g) ; $\frac{\partial |h_{pn}^{sh}(s)|}{\partial z}$ and
 208 $\frac{\partial^2 |h_{pn}^{sh}(s)|}{\partial z^2}$ are the first and second-order partial derivatives of $|h_{pn}^{sh}(s)|$ with respect to z ,
 209 ($z = c_h$ or k_h), respectively.

210 Similarly, the expectation and standard deviation of the phase can be expressed as,

$$211 \quad E(\angle h_{pn}^{sh}(s)) \approx \angle h_{pn}^{sh}(s) \Big|_{\substack{c_h=E_{c_h} \\ k_h=E_{k_h}}} + \frac{1}{2} \left(\frac{\partial^2 \angle h_{pn}^{sh}(s)}{\partial c_h^2} \Big|_{\substack{c_h=E_{c_h} \\ k_h=E_{k_h}}} \sigma_{c_h}^2 + \frac{\partial^2 \angle h_{pn}^{sh}(s)}{\partial k_h^2} \Big|_{\substack{c_h=E_{c_h} \\ k_h=E_{k_h}}} \sigma_{k_h}^2 \right) \quad (20)$$

212 and

$$\sigma(\angle h_{pn}^{sh}(s)) \approx \sqrt{\left(\frac{\partial \angle h_{pn}^{sh}(s)}{\partial c_h}\bigg|_{c_h=E_{c_h}, k_h=E_{k_h}}\right)^2 \sigma_{c_h}^2 + \left(\frac{\partial \angle h_{pn}^{sh}(s)}{\partial k_h}\bigg|_{c_h=E_{c_h}, k_h=E_{k_h}}\right)^2 \sigma_{k_h}^2} \quad (21)$$

2.3. Numerical example: 2DOF human-structure system

Let us consider a SDOF structure occupied by a SDOF human shown in Fig. 1. The dynamic properties of the individual human and the structure as well as those of the human-structure system (obtained from eigenvalue analysis of the 2DOF model) are given in Table 1. The first vibration mode of the human-structure system having frequency f_1 and damping ratio ζ_1 is dominated by structural motion. The second mode (frequency f_2 and damping ratio ζ_2) is dominated by human motion.

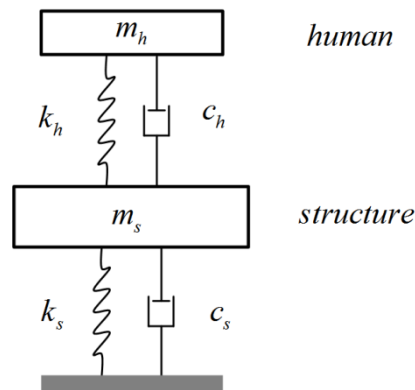


Fig. 1 2DOF model of human-structure system

If the direct receptance of the empty structure were measured accurately, it would have resulted in

$$h_{11}^s(s) = \frac{1}{m_s s^2 + c_s s + k_s} = \frac{1}{650s^2 + 792.31s + 6.04 \times 10^5} \quad (22)$$

226 Taking into account that the mass, damping and stiffness of the human body are $m_h = 62$ kg,
 227 $c_h = 1.44 \times 10^3$ N·s·m⁻¹ and $k_h = 6.12 \times 10^4$ N·m⁻¹, respectively, the direct receptance of the
 228 human-structure system $h_{11}^{sh}(s)$ can be calculated from Eq. (14)

$$229 \quad h_{11}^{sh}(s) = \frac{1}{650s^2 + 792.31s + 6.04 \times 10^5} - \frac{(1.44 \times 10^3 s + 6.12 \times 10^4) \left(\frac{1}{650s^2 + 792.31s + 6.04 \times 10^5} \right)^2}{1 + (1.44 \times 10^3 s + 6.12 \times 10^4) \left(\frac{1}{650s^2 + 792.31s + 6.04 \times 10^5} + \frac{1}{62s^2} \right)} \quad (23)$$

230 The characteristic equation

$$231 \quad 1 + (1.44 \times 10^3 s + 6.12 \times 10^4) \left(\frac{1}{650s^2 + 792.31s + 6.04 \times 10^5} + \frac{1}{62s^2} \right) = 0 \quad (24)$$

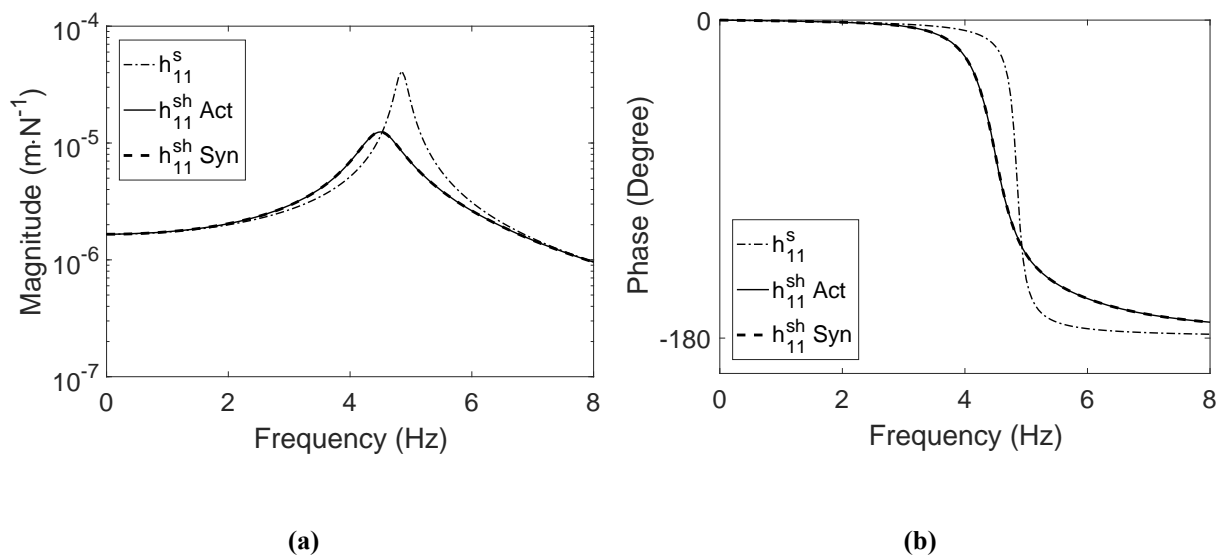
232 generates the eigenvalues of the human-structure system $\mu_{1,3} = -2.0595 \pm 28.2310i$ s⁻¹ and
 233 $\mu_{2,4} = -11.2826 \pm 31.8841i$ s⁻¹, which are the same as those shown in Table 1.

234 **Table 1 Dynamic properties of the human-structure system**

Dynamic property	Empty structure	Human*	Human-structure system
Mass (kg)	$m_s = 650$	$m_h = 62$	/
Damping (N·s·m ⁻¹)	$c_s = 792.31$	$c_h = 1.44 \times 10^3$	/
Stiffness (N·m ⁻¹)	$k_s = 6.04 \times 10^5$	$k_h = 6.12 \times 10^4$	/
Frequency (Hz)	$f_s = 4.85$	$f_s = 5.0$	$f_1 = 4.51, f_2 = 5.38$
Damping ratio (%)	$\zeta_s = 2.0$	$\zeta_s = 37.0$	$\zeta_1 = 7.3, \zeta_2 = 33.4$
Eigenvalues (s ⁻¹)	/	/	$\mu_{1,3} = -2.0595 \pm 28.2310i$ $\mu_{2,4} = -11.2826 \pm 31.8841i$
Eigenvectors	/	/	$\mathbf{v}_{1,3} = [0.3747 \pm 0.3132i \quad 1]$ $\mathbf{v}_{2,4} = [-0.0960 \pm 0.1282i \quad 1]$

235 * The human dynamic properties correspond to the fundamental mode of the human model
 236 for standing posture specified in ISO 5982 [33].

237 The synthesised direct receptance of the human-structure system described by Eq. (23),
 238 shown as the thick dashed line in Fig. 2, accurately reproduces the actual receptance of the
 239 human-structure system shown as the thin solid line. Fig. 2 also shows that the presence of
 240 the human shifts the frequency from 4.85 Hz for the empty structure (dash-dotted line) to
 241 4.51 Hz for the human-structure system. It also significantly increases the damping ratio of
 242 the mode dominated by structural motion (from 2.0% to 7.3%). The mode dominated by
 243 human motion is heavily damped which is the reason that it cannot be observed in the
 244 receptance graph for the human-structure system. The structure in this example is an actual
 245 16.9 m long glass FRP composite bridge [34]. The example demonstrates that the presence of
 246 a single human can significantly modify the dynamics of the empty structure.



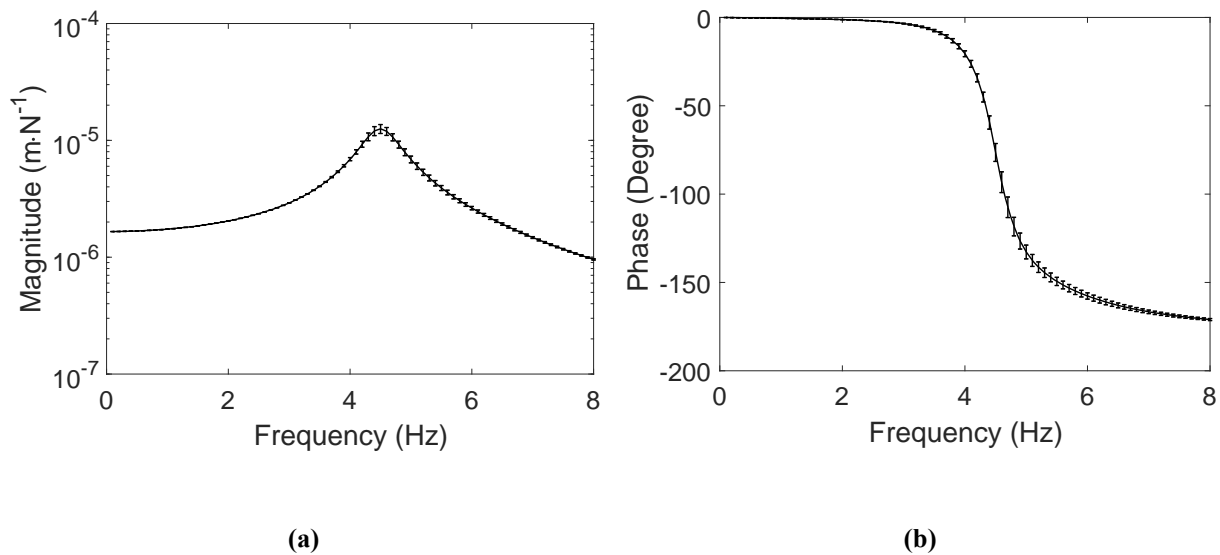
247 **Fig. 2 Receptances of the human-structure system and the structure: (a) Magnitude; (b) Phase**

248 Let us assume the expectation and standard deviation of the damping of the human body are

249 $E_{c_h} = 1.44 \times 10^3 \text{ N}\cdot\text{s}\cdot\text{m}^{-1}$ and $\sigma_{c_h} = 0.1c_h \text{ N}\cdot\text{s}\cdot\text{m}^{-1}$, respectively, while the counterparts for the

250 stiffness are $E_{k_h} = 6.12 \times 10^4 \text{ N}\cdot\text{m}^{-1}$ and $\sigma_{k_h} = 0.1k_h \text{ N}\cdot\text{m}^{-1}$ (The corresponding expectations

251 and standard deviations of the frequency and damping ratio are $E_{f_h} = 5.0\text{Hz}$ and $\sigma_{f_h} = 0.25$
252 Hz and $E_{\zeta_h} = 37.0\%$ and $\sigma_{\zeta_h} = 4.0\%$, estimated using the second-order perturbation method
253 [32]). By using the proposed uncertainty estimation method in Section 2.2, the expectation
254 and standard deviation of the direct receptance of the human-structure system can be obtained,
255 as plotted in Fig. 3. The coefficient of variation (CoV) of 10% for both the damping and
256 stiffness of the human body led to the maximum CoV of 9% for the magnitude and phase of
257 the predicted FRF of the human-structure system. The predicted expectations and standard
258 deviations shown in Fig. 3 were verified using Monte Carlo simulations (sample size = 1000).



259 **Fig. 3 The direct receptance of the human-structure system: (a) Magnitude; (b) Phase;**
260 **Solid line - Expectation; Error bar - Standard deviation**

261 3. Identification of the dynamics of the human body

262 In this section, formulas for identifying the dynamics of a stationary human occupying a
263 structure are presented, and their use is demonstrated in an experiment conducted on a
264 laboratory bridge.

265 3.1. Theoretical derivations

266 Let us assume that the direct receptance at the n -th DOF h_{nn}^s of the empty structure is
 267 available (for example, through modal testing). In addition, let us assume that the direct
 268 receptance at the n -th DOF or the cross receptance between the p -th output and the n -th input
 269 of the human-structure system is also available resulting in identifying the complex conjugate
 270 eigenvalues μ_k^{sh} and $\bar{\mu}_k^{sh}$ of the k -th mode dominated by structural motion of the human-
 271 structure system. The eigenvalues μ_k^{sh} and $\bar{\mu}_k^{sh}$ should satisfy Eq. (15), i.e.

$$272 \begin{bmatrix} c_h \\ k_h \end{bmatrix} = \begin{bmatrix} \mu_k^{sh} & 1 \\ \bar{\mu}_k^{sh} & 1 \end{bmatrix}^{-1} \begin{bmatrix} \frac{(\mu_k^{sh})^2 m_h}{(\mu_k^{sh})^2 m_h h_{nn}^s (\mu_k^{sh}) + 1} \\ \frac{(\bar{\mu}_k^{sh})^2 m_h}{(\bar{\mu}_k^{sh})^2 m_h h_{nn}^s (\bar{\mu}_k^{sh}) + 1} \end{bmatrix} \quad (25)$$

273 Eq. (25) demonstrates that the damping c_h and stiffness k_h of the human can be calculated
 274 using the mass of the human m_h and the direct receptance of the empty structure $h_{nn}^s(s)$ that
 275 is evaluated at a pair of eigenvalues μ_k^{sh} and $\bar{\mu}_k^{sh}$. Eq. (25) always results in real solutions for
 276 c_h and k_h due to the use of the complex conjugate pair μ_k^{sh} and $\bar{\mu}_k^{sh}$.

277 Making use of the proposed approach for experimental identification of human properties is
 278 straightforward. It only requires measuring a direct receptance for the empty structure and a
 279 direct receptance or a cross receptance for the human-structure system.

280 If the measured quantity is accelerance rather than receptance, an alternative form of Eq. (25)
 281 should be used. The acceleration $\mathbf{a}(s)$ and the displacement $\mathbf{x}(s)$ are related via

282 $\mathbf{a}(s) = s^2 \mathbf{x}(s)$. The receptance matrix $\mathbf{H}^s(s)$ and the accelerance matrix $\mathbf{H}_a^s(s)$ satisfy the
 283 relationship

$$284 \quad \mathbf{H}^s(s) = \frac{\mathbf{H}_a^s(s)}{s^2} \quad (26)$$

285 leading to the estimate of the damping and stiffness of the human from Eq. (27)

$$286 \quad \begin{bmatrix} c_h \\ k_h \end{bmatrix} = \begin{bmatrix} \mu_k^{sh} & 1 \\ \bar{\mu}_k^{sh} & 1 \end{bmatrix}^{-1} \begin{bmatrix} \frac{(\mu_k^{sh})^2 m_h}{m_h h_{a,nn}^s(\mu_k^{sh}) + 1} \\ \frac{(\bar{\mu}_k^{sh})^2 m_h}{m_h h_{a,nn}^s(\bar{\mu}_k^{sh}) + 1} \end{bmatrix} \quad (27)$$

287 As can be seen from Eqs. (25) and (27), the identification of human body dynamics relies on
 288 the quality of the curve fitting of the FRFs of the empty structure and also of the FRFs around
 289 the modes dominated by structural motion of the joint system. The strategies for performing
 290 curve fitting have been investigated elsewhere, e.g. [35, 36], and have not been elaborated in
 291 this paper.

292 **3.2. Experimental case study: Dynamic properties of a human in a standing posture**

293 The use of the proposed method is demonstrated on an example of identifying the dynamic
 294 properties of a human standing on a steel-concrete composite bridge situated in the Structures
 295 Laboratory at the University of Warwick (Fig. 4). The bridge has a mass of 16,500 kg whilst
 296 its deck is 19.9 m long and 2 m wide. It sits on two meccano frames that span 16.34 m. The
 297 mass of the human is 100 kg and his height is 180 cm. The experiments were approved by the
 298 Biomedical and Scientific Research Ethics Committee at the University of Warwick.

299 Accelerances of the empty bridge and the human-bridge system were measured in a modal
300 testing programme. The measurement points are shown in Fig. 5. The bridge was excited
301 using an electrodynamic shaker (Model APS 400) placed at test point (TP) 1, as shown in Fig.
302 6. The generated force was indirectly measured using an accelerometer (Honeywell QA750)
303 of nominal sensitivity 1300 mV/g attached to the moving armature. Another two
304 accelerometers of the same type were placed at TP1 and TP2 to measure the vibration
305 responses of the bridge in the vertical direction. The data acquisition system consisted of a
306 laptop, a 4-channel data logger (SignalCalc Ace by Data Physics), a signal conditioner and a
307 power amplifier (Model APS 145). A chirp signal in the frequency range 1-9 Hz was applied
308 to the structure for 64 seconds. A data acquisition window was set to 128 seconds. No
309 window was used in data processing since the vibration responses returned to the ambient
310 level within the data acquisition window. Six averages were used to minimise the effects of
311 noise. The typical standing posture of the human is shown in Fig. 6.

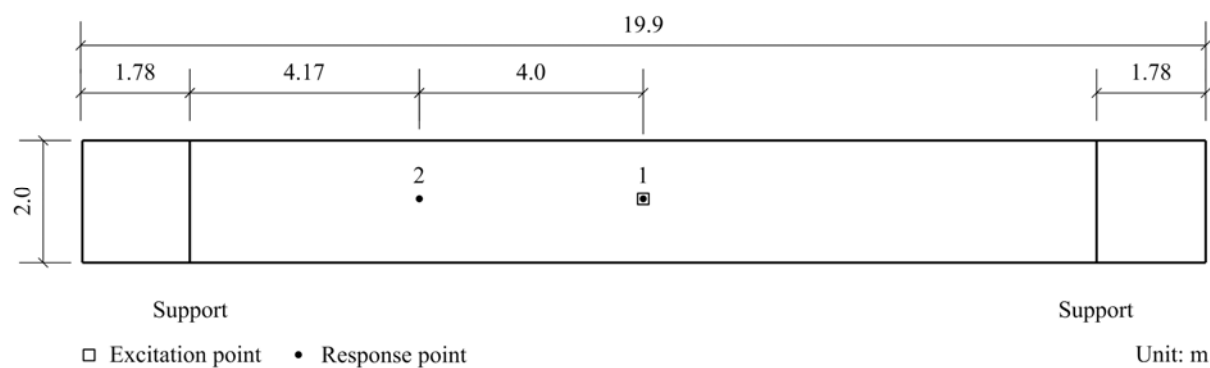


312

Fig. 4 The empty structure

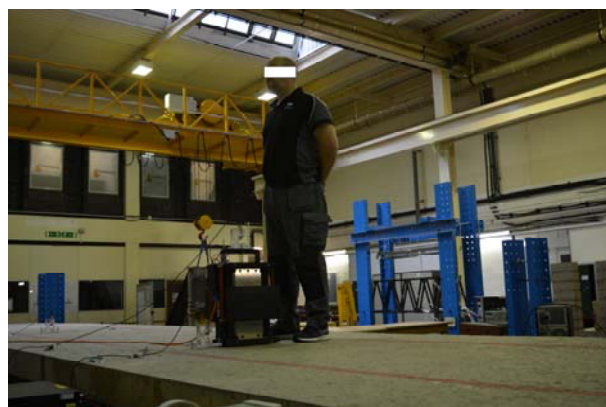
313

314



316 **Fig. 5 Bridge geometry and measurement points**

317



318

319 **Fig. 6 A human and a shaker at TP1**

320 **3.2.1. Modal testing**

321 The dynamic properties of the human body were identified at three different force levels. The
322 induced maximum accelerations at the driving point on the empty bridge and the human-
323 bridge system ranged from $0.36 \text{ m}\cdot\text{s}^{-2}$ to $0.65 \text{ m}\cdot\text{s}^{-2}$ and from $0.34 \text{ m}\cdot\text{s}^{-2}$ to $0.62 \text{ m}\cdot\text{s}^{-2}$,
324 respectively. The frequencies and damping ratios of the empty structure showed negligible
325 variation with the response level. The same conclusion was drawn for the human-structure
326 system. These findings suggest that the empty bridge and the human-bridge system exhibited
327 relatively linear behaviour at the three different force levels and they all resulted in almost the
328 same properties of the human body. The force level chosen for presentation in this paper is
329 shown in Fig. 7 whilst the corresponding vibration response at TP1 for the unoccupied bridge

330 is shown in Fig. 8. The direct and cross accelerances for the empty bridge and the bridge
 331 occupied by the test subject are shown in Fig. 9 and Fig. 10, respectively. The two figures
 332 show that the presence of the test subject affects the dynamics of the system slightly.

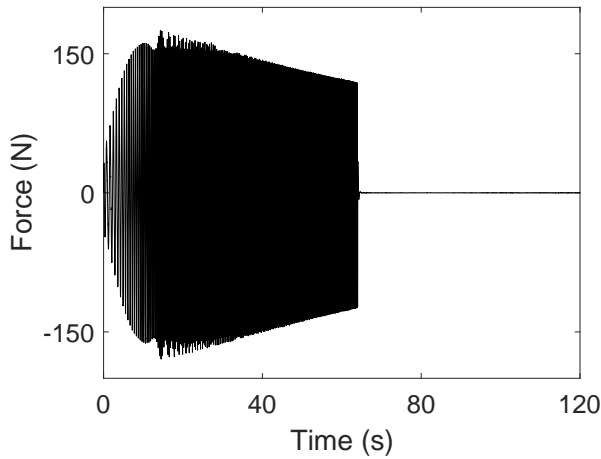


Fig. 7 Excitation force at TP1

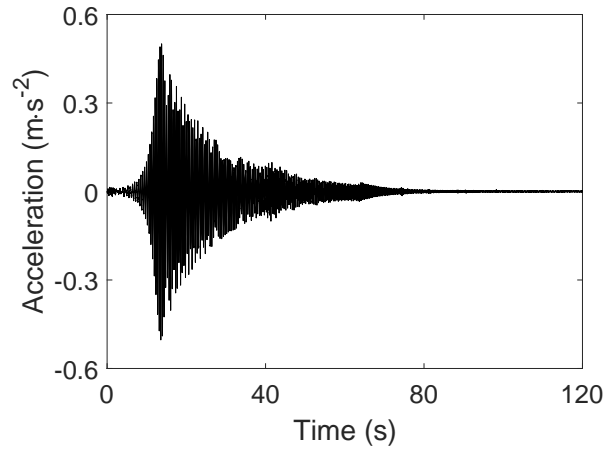
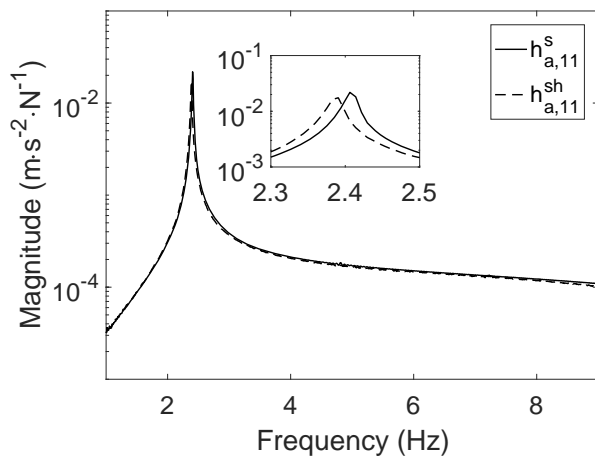
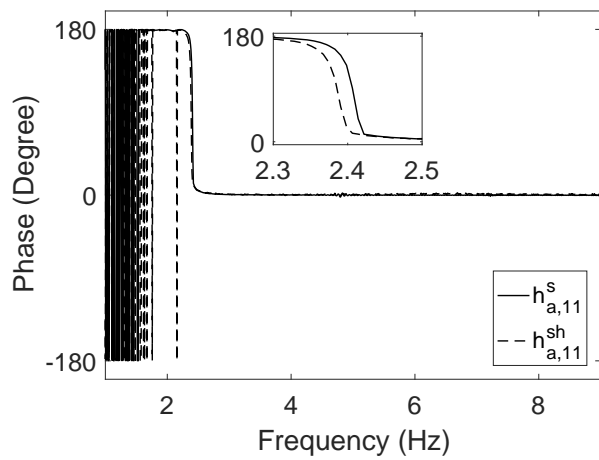


Fig. 8 Acceleration at TP1

333



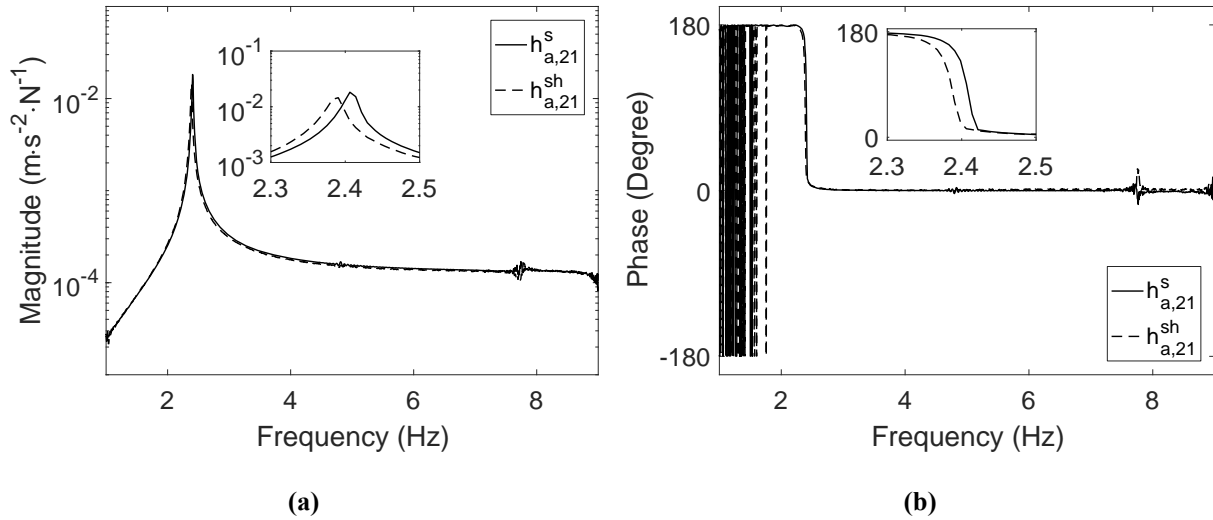
(a)



(b)

334

Fig. 9 Direct accelerances of the unoccupied and occupied structures: (a) Magnitude; (b) Phase

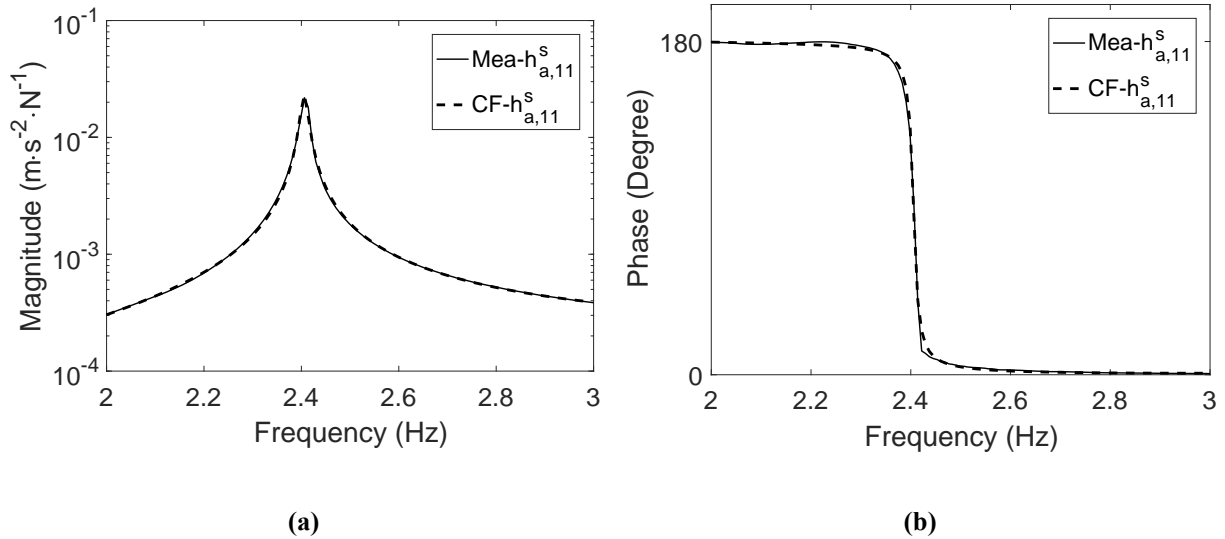


335 **Fig. 10 Cross accelerances of the unoccupied and occupied structures: (a) Magnitude; (b) Phase**
 336 The measured acceleration $h_{a,11}^s$ of the empty structure was curve fitted using the rational
 337 fraction polynomial method [35]. Good agreement between the curve-fitted (CF)
 338 accelerance and its measured counterpart is demonstrated in Fig. 11. The analytical
 339 expression of the curve-fitted accelerance is

$$340 \quad h_{a,11}^s(s) = \frac{a_0 s^6 + a_1 s^5 + a_2 s^4 + a_3 s^3 + a_4 s^2 + a_5 s + a_6}{b_0 s^2 + b_1 s + b_2} \quad (28)$$

341 where $a_0 = 2.0486 \times 10^{-9} \text{ s}^4$, $a_1 = -2.9053 \times 10^{-9} \text{ s}^3$, $a_2 = 1.4985 \times 10^{-6} \text{ s}^2$,
 342 $a_3 = -1.6243 \times 10^{-6} \text{ s}$, $a_4 = -5.9928 \times 10^{-4}$, $a_5 = -2.1540 \times 10^{-4} \text{ s}^{-1}$, $a_6 = 0.0266 \text{ s}^{-2}$,
 343 $b_0 = 1.8069 \text{ N} \cdot \text{s}^2 \cdot \text{m}^{-1}$, $b_1 = 0.1606 \text{ N} \cdot \text{s} \cdot \text{m}^{-1}$ and $b_2 = 412.8475 \text{ N} \cdot \text{m}^{-1}$.

344 The pair of eigenvalues corresponding to the first mode of the human-structure system were
 345 identified to be $-0.0536 \pm 14.9840i \text{ s}^{-1}$ by curve fitting either the accelerance $h_{a,11}^{sh}$ or $h_{a,21}^{sh}$.

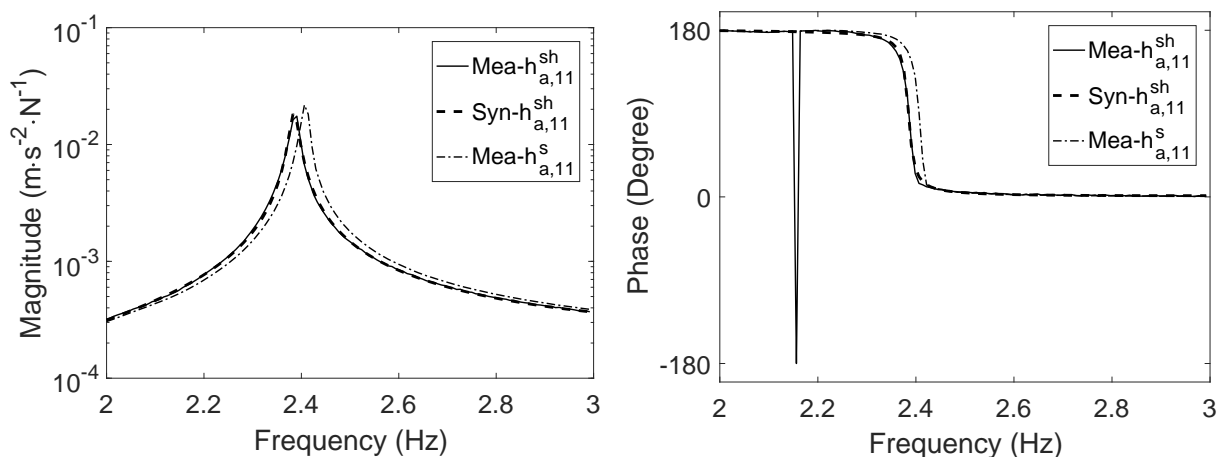


346 Fig. 11 Comparison between measured and curve-fitted accelerance $h_{a,11}^s$: (a) Magnitude; (b) Phase

347 **3.2.2. Dynamic properties of the human body**

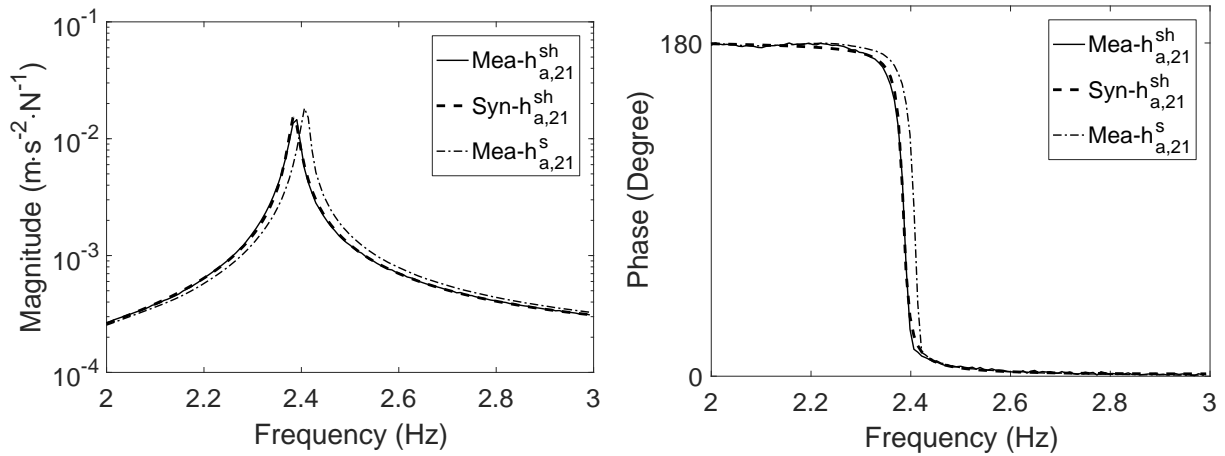
348 Based on the direct accelerance of the empty structure (Eq. (28)), the pair of eigenvalues of
 349 the occupied bridge and Eq. (27), the undamped frequency and damping ratio of the test
 350 subject were identified to be 4.85 Hz and 27.0%, respectively.

351 To validate the results, the accelerances $h_{a,21}^{sh}$ and $h_{a,11}^{sh}$ were synthesised using Eqs. (13) and
 352 (14). Fig. 12 and Fig. 13 show that the synthesised accelerances (thick dashed curves) of the
 353 human-structure system agree well with their measured counterparts (thin solid curves).



354

(a) (b)
Fig. 12 Direct accelerances of unoccupied and occupied structures: (a) Magnitude; (b) Phase



(a) (b)

355 **Fig. 13 Cross accelerances of unoccupied and occupied structures: (a) Magnitude; (b) Phase**

356 To further validate the results of the identification of human body dynamics, the nonlinear
 357 optimisation method [2] was employed. The natural frequency identified in this way was 4.84
 358 Hz and damping ratio was 30.0%. These results are close to those identified by the proposed
 359 method, confirming its validity.

360 3.2.3. Discussion on the working of the method for identifying the dynamics of the 361 human body

362 According to Eq. (27), theoretically, if the eigenvalues μ_k^{sh} and $\bar{\mu}_k^{sh}$ of the human-structure
 363 system are different from the eigenvalues μ_k^s and $\bar{\mu}_k^s$ of the empty structure, the damping and
 364 stiffness of the human can be identified. In practice, only a reliable detection of the
 365 eigenvalue difference between the unoccupied and occupied structures leads to reliable
 366 damping and stiffness. The eigenvalue difference is composed of the frequency and damping
 367 differences, which correspond to the changes of the peak frequency and magnitude of FRF,
 368 respectively. Hence, the working of the proposed method relies on the reliable detection of
 369 the changes of the peak frequency and magnitude of FRF.

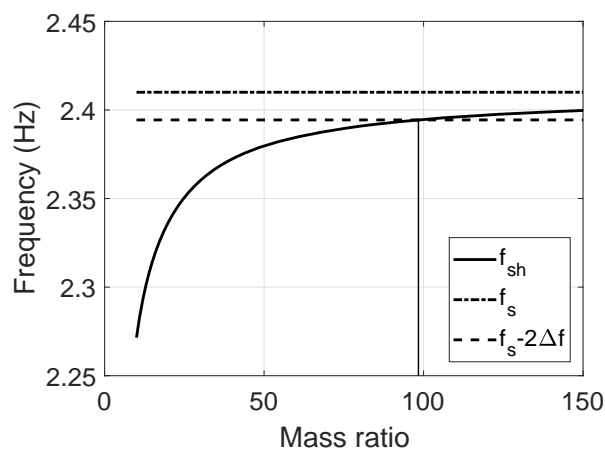
370 A conservative criterion for reliable identification of two closely spaced spectral peaks states
371 that the frequency separation between the two peaks should be at least twice the frequency
372 resolution provided the rectangular window is used in signal processing [37]. The frequency
373 separation is required to be four times greater than the frequency resolution in cases in which
374 the Hann or Hamming window is used [37]. Therefore, the proposed method allows the
375 reliable identification of human body dynamics if the frequency difference between the
376 unoccupied and occupied structures is at least two times greater than the frequency resolution
377 when the rectangular window is used in data processing or at least four times greater when
378 the Hann or Hamming window is utilised.

379 Since the rectangular window was used in analysis of the human-structure system presented
380 in Section 3.2 and the frequency separation of 0.03 Hz is approximately four times of the
381 frequency resolution ($\Delta f = 1/128$ Hz), the identification of the human body dynamics is
382 reliable in the example presented.

383 The structure (modal) to human mass ratio is one of the factors which affects the frequency
384 difference [9]. Based on the criterion about the minimum frequency difference, the effect of
385 the mass ratio may be investigated using parametric analysis. Let us consider the human-
386 structure system presented in Section 3.2. Let us assume that the bridge has frequency of 2.41
387 Hz, damping ratio of 0.3% and varying modal mass while the properties of the human are as
388 follows: mass 100kg, frequency 4.85Hz and damping ratio 27.0%. The frequency of the
389 mode dominated by the structural motion of the joint system can be calculated (thick solid
390 line in Fig. 14). The thick dashed line in Fig. 14 is separated by a distance of $2\Delta f (=0.0156$
391 Hz) from the thick dash-dotted line, which indicates the frequency of the unoccupied system
392 (2.41 Hz). The intersection of the thick solid line and the thick dashed line indicates that the
393 frequency difference is greater than $2\Delta f$ for the mass ratio up to 98. For the human-structure

394 system presented in Section 3.2, the mass ratio was 70, and therefore the human body
395 dynamics were reliably identifiable.

396 The structure to human ratios for frequency and damping ratio are the other two factors
397 affecting the frequency difference [9]. The parametric analysis for investigating the effect of
398 the structure to human ratios for frequency and damping ratio is similar to that for the mass
399 ratio and therefore it is not presented here.



400

401 **Fig. 14 Frequency of the mode dominated by structural motion against the modal mass of the structure to**
402 **the human mass ratio ($\Delta f = 1/128$)**

403 **4. Identification of the dynamics of the empty structure**

404 In this section, formulas for the identification of the properties of the empty structure from
405 the known dynamics of the human and human-structure system are presented. Their use is
406 illustrated utilising the experiment described in Section 3.2 and a numerical example of a
407 three-span glass FRP composite bridge.

408 **4.1. Theoretical derivations**

409 Rearranging Eq. (14) generates the direct receptance of the unoccupied structure

$$410 \quad h_{nn}^s(s) = \frac{\left(1 + \frac{1}{m_h s^2} (c_h s + k_h)\right) h_{nn}^{sh}(s)}{1 + \frac{1}{m_h s^2} (c_h s + k_h) - (c_h s + k_h) h_{nn}^{sh}(s)} \quad (29)$$

411 which is a function of the known direct receptance $h_{nn}^{sh}(s)$ of the human-structure system and
 412 the known dynamic properties of the human.

413 Rewriting (13) leads to

$$414 \quad h_{pn}^s(s) = h_{pn}^{sh}(s) + \frac{h_{nn}^s(s)(c_h s + k_h) h_{pn}^{sh}(s)}{\left(1 + \frac{1}{m_h s^2} (c_h s + k_h)\right)} \quad (30)$$

415 Substituting (29) into (30) results in

$$416 \quad h_{pn}^s(s) = h_{pn}^{sh}(s) + \frac{h_{pn}^{sh}(s)(c_h s + k_h) h_{nn}^{sh}(s)}{1 + \frac{1}{m_h s^2} (c_h s + k_h) - (c_h s + k_h) h_{nn}^{sh}(s)} \quad (31)$$

417 which shows that the cross receptance of the unoccupied structure could be deduced from the
 418 direct and cross receptance functions of the human-structure system and the dynamic
 419 properties of the human. The natural frequency and damping ratio of the unoccupied structure
 420 can then be calculated from the characteristic equation (i.e. denominator in Eqs. (29) or (31)
 421 equated to zero).

422 As can be seen from Eqs. (29) and (31), the quality of the curve fitting of the FRFs around
 423 the modes dominated by structural motion of the joint system plays a key role in identifying

424 the modes of the empty structure. The strategies for performing curve fitting have been
 425 investigated elsewhere, e.g. [35, 36], and have not been elaborated in this paper.

426 **4.2. The effect of uncertainties in the human body dynamics on the identification of the**
 427 **dynamic properties of the empty structure**

428 The expectation and standard deviation of the magnitude of the pn -th receptance of the empty
 429 structure system can be expressed as

$$430 \quad E\left(|h_{pn}^s(s)|\right) \approx |h_{pn}^s(s)|_{\substack{c_h=E_{c_h} \\ k_h=E_{k_h}}} + \frac{1}{2} \left(\frac{\partial^2 |h_{pn}^s(s)|}{\partial c_h^2} \bigg|_{\substack{c_h=E_{c_h} \\ k_h=E_{k_h}}} \sigma_{c_h}^2 + \frac{\partial^2 |h_{pn}^s(s)|}{\partial k_h^2} \bigg|_{\substack{c_h=E_{c_h} \\ k_h=E_{k_h}}} \sigma_{k_h}^2 \right) \quad (32)$$

431 and

$$432 \quad \sigma\left(|h_{pn}^s(s)|\right) \approx \sqrt{\left(\frac{\partial |h_{pn}^s(s)|}{\partial c_h} \bigg|_{\substack{c_h=E_{c_h} \\ k_h=E_{k_h}}} \right)^2 \sigma_{c_h}^2 + \left(\frac{\partial |h_{pn}^s(s)|}{\partial k_h} \bigg|_{\substack{c_h=E_{c_h} \\ k_h=E_{k_h}}} \right)^2 \sigma_{k_h}^2} \quad (33)$$

433 Similarly, the expectation and standard deviation of the phase of the pn -th receptance of the
 434 empty structure system can be expressed as,

$$435 \quad E\left(\angle h_{pn}^s(s)\right) \approx \angle h_{pn}^s(s) \bigg|_{\substack{c_h=E_{c_h} \\ k_h=E_{k_h}}} + \frac{1}{2} \left(\frac{\partial^2 \angle h_{pn}^s(s)}{\partial c_h^2} \bigg|_{\substack{c_h=E_{c_h} \\ k_h=E_{k_h}}} \sigma_{c_h}^2 + \frac{\partial^2 \angle h_{pn}^s(s)}{\partial k_h^2} \bigg|_{\substack{c_h=E_{c_h} \\ k_h=E_{k_h}}} \sigma_{k_h}^2 \right) \quad (34)$$

436 and

$$437 \quad \sigma\left(\angle h_{pn}^s(s)\right) \approx \sqrt{\left(\frac{\partial \angle h_{pn}^s(s)}{\partial c_h} \bigg|_{\substack{c_h=E_{c_h} \\ k_h=E_{k_h}}} \right)^2 \sigma_{c_h}^2 + \left(\frac{\partial \angle h_{pn}^s(s)}{\partial k_h} \bigg|_{\substack{c_h=E_{c_h} \\ k_h=E_{k_h}}} \right)^2 \sigma_{k_h}^2} \quad (35)$$

438 4.3. Experimental case study: Dynamic properties of the structure

439 The use of the proposed method is demonstrated on an example of identifying the properties
 440 of the bridge from Section 3.2, by utilising the measured accelerances while the test subject
 441 was standing on the structure and known properties of the human. The measured direct and
 442 cross accelerances were curve fitted using the rational fraction polynomial method [35]. The
 443 analytical expression of the curve-fitted acceleration $h_{a,11}^{sh}(s)$ is

$$444 \quad h_{a,11}^{sh}(s) = \frac{a_0 s^6 + a_1 s^5 + a_2 s^4 + a_3 s^3 + a_4 s^2 + a_5 s + a_6}{b_0 s^2 + b_1 s + b_2} \quad (36)$$

445 where $a_0 = 1.8385 \times 10^{-9} \text{ s}^4$, $a_1 = -1.7167 \times 10^{-9} \text{ s}^3$, $a_2 = 1.3257 \times 10^{-6} \text{ s}^2$,
 446 $a_3 = -9.7898 \times 10^{-7} \text{ s}$, $a_4 = 5.5414 \times 10^{-4}$, $a_5 = -1.4522 \times 10^{-4} \text{ s}^{-1}$, $a_6 = 0.0228 \text{ s}^{-2}$,
 447 $b_0 = 1.8417 \text{ N} \cdot \text{s}^2 \cdot \text{m}^{-1}$, $b_1 = 0.1975 \text{ N} \cdot \text{s} \cdot \text{m}^{-1}$ and $b_3 = 413.5110 \text{ N} \cdot \text{m}^{-1}$.

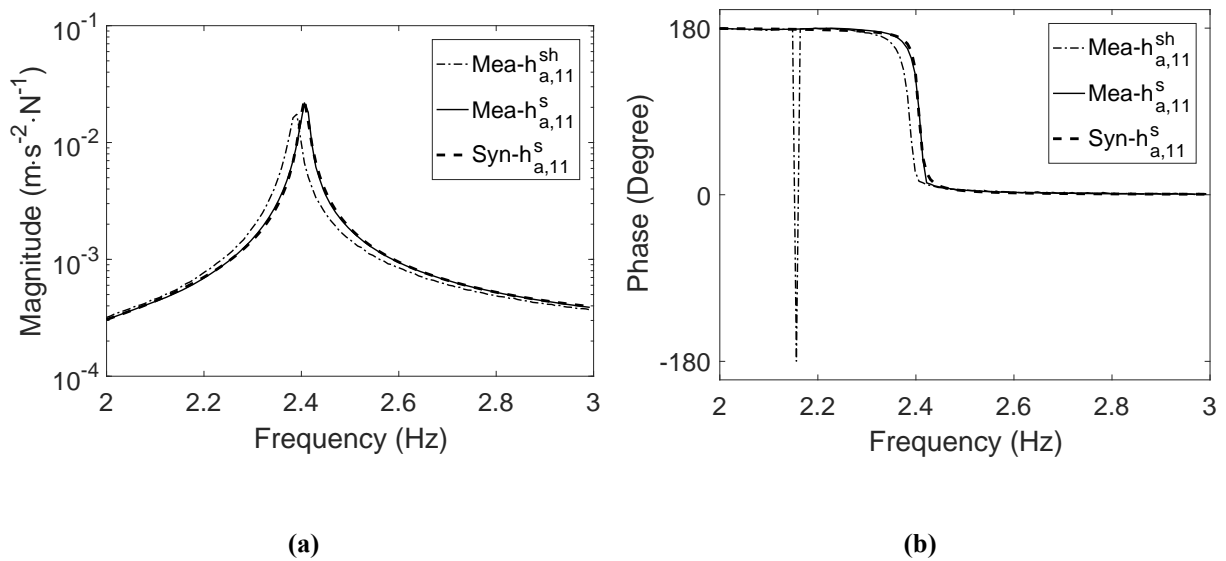
448 The analytical expression of the curve-fitted accelerance $h_{a,21}^{sh}(s)$ is

$$449 \quad h_{a,21}^{sh}(s) = \frac{a_0 s^6 + a_1 s^5 + a_2 s^4 + a_3 s^3 + a_4 s^2 + a_5 s + a_6}{b_0 s^2 + b_1 s + b_2} \quad (37)$$

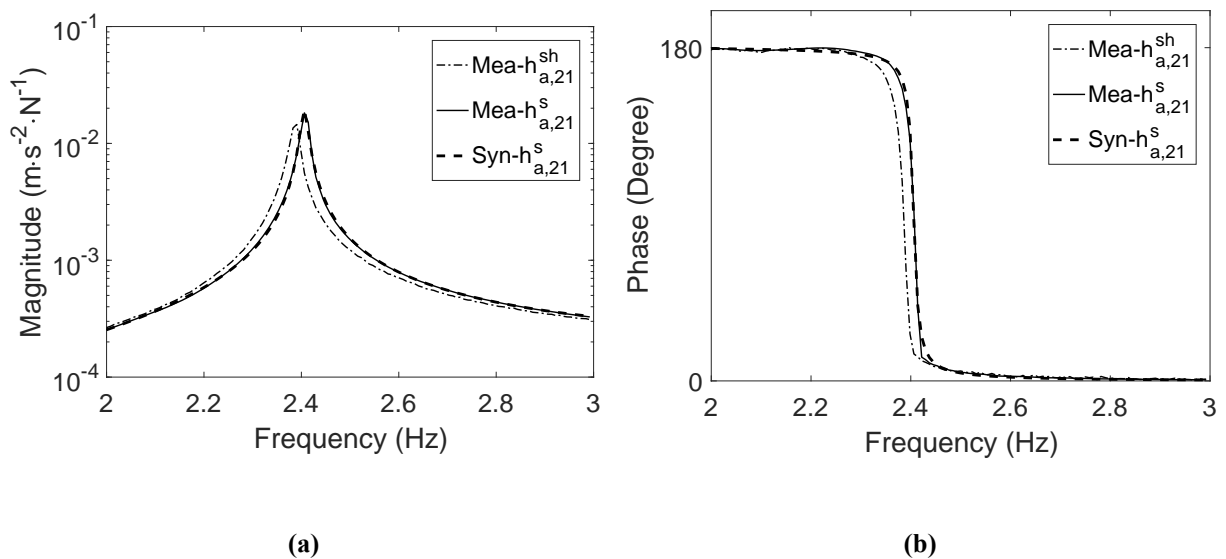
450 where $a_0 = 1.8438 \times 10^{-9} \text{ s}^4$, $a_1 = -1.6904 \times 10^{-9} \text{ s}^3$, $a_2 = 1.3114 \times 10^{-6} \text{ s}^2$,
 451 $a_3 = -9.6580 \times 10^{-7} \text{ s}$, $a_4 = 5.4878 \times 10^{-4}$, $a_5 = -1.4277 \times 10^{-4} \text{ s}^{-1}$, $a_6 = 0.0225 \text{ s}^{-2}$,
 452 $b_0 = 2.2058 \text{ N} \cdot \text{s}^2 \cdot \text{m}^{-1}$, $b_1 = 0.2366 \text{ N} \cdot \text{s} \cdot \text{m}^{-1}$ and $b_3 = 495.2469 \text{ N} \cdot \text{m}^{-1}$.

453 The accelerances $h_{a,11}^s$ and $h_{a,21}^s$ were then found using Eqs. (29) and (31). Fig. 15 and Fig. 16
 454 show that the calculated accelerances (thick dashed lines) of the empty structure agree well

455 with their measured counterparts (thin solid lines). Utilising the characteristic equation for the
 456 synthesised accelerances of the empty structure, the fundamental natural frequency and
 457 damping ratio of the empty structure were identified as 2.41 Hz and 0.3 % (i.e. the same
 458 values that would be obtained by curve fitting the measured accelerance for the empty
 459 structure).



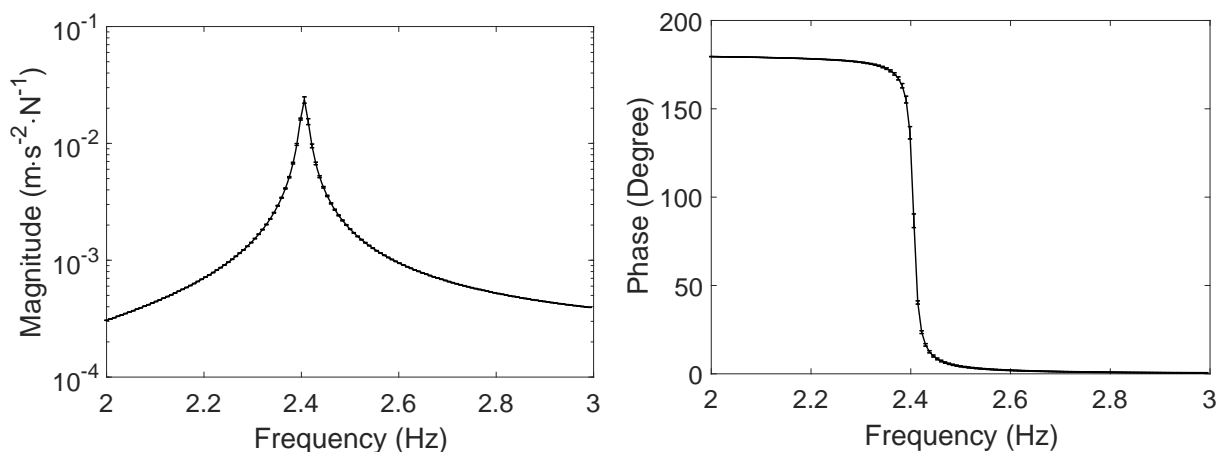
460 **Fig. 15 Direct accelerances of unoccupied and occupied structures: (a) Magnitude; (b) Phase**



461 **Fig. 16 Cross accelerances of unoccupied and occupied structures: (a) Magnitude; (b) Phase**

462 Let the expectations of the damping and stiffness of the human body be $E_{c_h} = 1.65 \times 10^3$
 463 $\text{N}\cdot\text{s}\cdot\text{m}^{-1}$ and $E_{k_h} = 9.28 \times 10^4 \text{ N}\cdot\text{m}^{-1}$, respectively. Let us assume that the standard deviations of
 464 the damping and stiffness are $\sigma_{c_h} = 0.1c_h \text{ N}\cdot\text{s}\cdot\text{m}^{-1}$ and $\sigma_{k_h} = 0.1k_h \text{ N}\cdot\text{m}^{-1}$, respectively. The
 465 corresponding expectations and standard deviations of the damping ratio and frequency of the
 466 human body are $E_{\zeta_h} = 27.0\%$ and $\sigma_{\zeta_h} = 3.0\%$ and $E_{f_h} = 4.84 \text{ Hz}$ and $\sigma_{f_h} = 0.24 \text{ Hz}$, estimated
 467 using the second-order perturbation method [32]. By using the proposed uncertainty
 468 estimation method, the expectation and standard deviation of the direct accelerance of the
 469 empty bridge are plotted in Fig. 17. The CoV of 10% for both the damping and stiffness of
 470 the human body led to the maximum CoV of 7% for the magnitude and phase of the
 471 predicted FRF of the empty structure. The predicted expectation and standard deviation of
 472 FRFs were verified using Monte Carlo simulations (sample size = 1000).

473



(a)

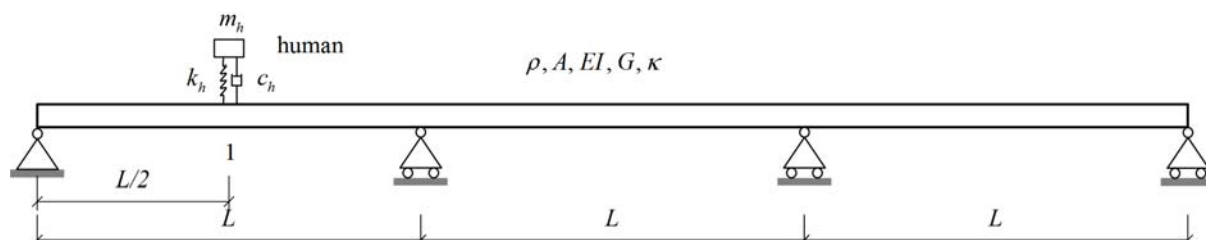
(b)

474 **Fig. 17 Direct accelerance of the empty system: (a) Magnitude; (b) Phase;**
 475 **Solid line - Expectation; Error bar - Standard deviation**

476 4.4. Numerical example: correcting multiple modes of a bridge

477 A three-span continuous bridge (Fig. 18) made of glass FRP composite material is used to
 478 illustrate the robustness of the method. The bridge has a total length of $3L = 3 \times 20 = 60$ m,
 479 density $\rho = 1.9 \times 10^3$ kg·m⁻³, area of cross section $A = 2.5 \times 10^{-2}$ m², longitudinal modulus of
 480 elasticity $E = 2.47 \times 10^{10}$ N·m⁻², second moment of area $I = 2.0 \times 10^{-3}$ m⁴, shear modulus
 481 $G = 3.9 \times 10^9$ N·m⁻² and shear coefficient $\kappa = 0.08$. A human having mass $m_h = 73$ kg,
 482 natural frequency $f_h = 4.41$ Hz and damping ratio $\zeta_h = 33.0\%$ is assumed to stand in the
 483 middle of the first span (point 1 in Fig. 18).

484 A two-dimensional finite element (FE) model of the bridge is developed using an improved
 485 two-node Timoshenko beam finite element [38]. The FE model consists of 120 elements of
 486 equal length. Proportional damping $\mathbf{C} = \alpha\mathbf{M} + \beta\mathbf{K}$ ($\alpha = \beta = 0.0006$) is assumed. Similarly,
 487 the FE model of the human-bridge system can be obtained.



488
 489 **Fig. 18 A three-span continuous bridge**

490 Numerical integration was first carried out to calculate the time-domain responses of the
 491 human-bridge system driven by a linear chirp excitation force (having magnitude 100 N and
 492 sweeping from 1 Hz to 10 Hz) at point 1 for 112 seconds and then left to return to rest over
 493 the next 8 seconds. The actual direct receptance h_{11}^{sh} of the human-bridge system was then
 494 numerically estimated using the excitation force and the resultant vertical displacement
 495 response at point 1 and it is shown by the thin dash-dotted line in Fig. 19. This receptance

496 plays the role of a known (usually by measurement) FRF of the human-structure system. By
497 curve fitting the receptance h_{11}^{sh} in the frequency range from 2 Hz to 8 Hz, a rational fraction
498 polynomial of the direct receptance may be obtained as

$$499 \quad h_{11}^{sh}(s) = \frac{\sum_{i=1}^{13} a_{i-1} s^{13-i}}{\sum_{j=1}^9 b_{j-1} s^{9-j}} \quad (38)$$

500 where a_{i-1} ($i=1,2,L,13$) and b_{j-1} ($j=1,2,L,9$) are given the appendix. Its characteristic
501 equation gives the natural frequencies and damping ratios of the first four modes of the
502 human-bridge system, which are summarised in Table 2.

503 By using the proposed method, the known human body dynamics, Eqs. (38) and (29), the
504 direct receptance of the unoccupied bridge in the frequency range from 2 Hz to 8 Hz can be
505 synthesised, shown by the thick dashed line in Fig. 19. It can be seen that the synthesised
506 receptance of the unoccupied bridge is coincident with the actual receptance (denoted as Act
507 in Fig. 19) of the unoccupied bridge (the thin solid line in Fig. 19), which was obtained
508 numerically. The natural frequencies and damping ratios of the unoccupied bridge were then
509 determined by solving the characteristic equation obtained from the synthesised direct
510 receptance of the unoccupied bridge and they are presented in Table 2.

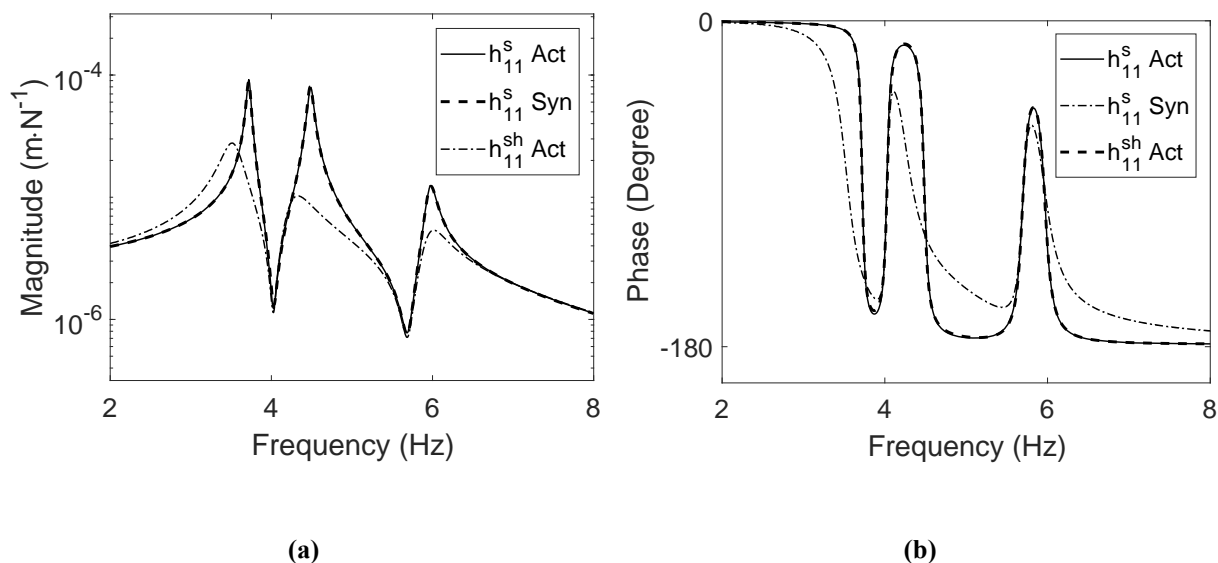


Fig. 19 Direct receptances of the occupied and unoccupied structures: (a) Magnitude; (b) Phase

511 **Table 2 Modal parameters of the human-bridge system and the unoccupied bridge (S Mode - Structural**
 512 **motion dominated mode; H Mode - Human motion dominated mode)**

No.	Mode Description	Human-bridge system		Empty bridge		Relative difference (%)	
		Frequency (Hz)	Damping ratio (%)	Frequency (Hz)	Damping ratio (%)	Frequency	Damping ratio
1	S Mode	3.53	3.8	3.72	0.7	-5.1	443
2	S Mode	4.25	4.1	4.48	0.8	-5.1	413
3	H Mode	5.00	23.8	/	/	/	/
4	S Mode	5.95	2.7	5.97	1.1	-0.3	145

513 The occupancy of the human increases the damping ratios of the first three structural motion
 514 dominated modes by 443%, 413% and 145%, respectively (Table 2). By contrast, it decreases
 515 the frequencies of the first three modes by 5.1%, 5.1% and 0.3%, respectively. This example
 516 demonstrates that had the measured human-structure receptances not been corrected, the
 517 modal properties of the structure would be erroneous.

518 Fig. 19 shows that the proposed method corrects the dynamic properties of the first three
 519 modes (two of which are relatively closely spaced) simultaneously which is advantageous
 520 compared with the methods that rely on SDOF models of the structure.

521 **5. Conclusions**

522 The paper presents a new theoretical framework which offers closed-form solutions in terms
523 of curve-fitted FRFs and flexibility of being used for any of the three applications as and
524 when needed, i.e. prediction of the dynamics of a structure occupied by a human when the
525 properties of individual components are known, the identification of human body dynamics
526 when the dynamics of the empty structure and the structure occupied by the human are
527 known and the identification of the empty structure when the dynamics of the human and the
528 structure occupied by the human are known. In addition, the influence of uncertainties in
529 human body dynamics on the dynamic identification of the empty structure and human-
530 structure system was quantified using the second-order perturbation method. The robustness
531 and accuracy of the proposed framework were demonstrated in several numerical and
532 experimental examples. The method is simple to use, it is computationally efficient and it
533 provides an effective means of studying human-structure interaction problems that are
534 especially relevant for light-weight, slender structures. The proposed method, which focuses
535 on the presence of a single human in this paper, will be extended to the crowd-structure
536 interaction in future work.

537 **ACKNOWLEDGMENT**

538 This research work was supported by the UK Engineering and Physical Sciences Research
539 Council [grant number EP/M021505/1: Characterising dynamic performance of fibre
540 reinforced polymer structures for resilience and sustainability]. The data are self-contained in
541 the paper.

542

543 Appendix : Coefficients in Eq. (38)

544 $a_0 = -2.1394 \times 10^{-23} \text{ s}^{10}$, $a_1 = 5.0748 \times 10^{-21} \text{ s}^9$, $a_2 = -9.3199 \times 10^{-19} \text{ s}^8$, $a_3 = 3.8819 \times 10^{-17}$
 545 s^7 , $a_4 = 2.5281 \times 10^{-15} \text{ s}^6$, $a_5 = 2.6507 \times 10^{-13} \text{ s}^5$, $a_6 = 1.1073 \times 10^{-10} \text{ s}^4$, $a_7 = 2.2661 \times 10^{-9} \text{ s}^3$,
 546 $a_8 = 2.8389 \times 10^{-07} \text{ s}^2$, $a_9 = 3.6935 \times 10^{-6} \text{ s}$, $a_{10} = 2.4034 \times 10^{-4}$, $a_{11} = 0.0015 \text{ s}^{-1}$, $a_{12} = 0.0658$
 547 s^{-2} , $b_0 = 4.4691 \times 10^{-8} \text{ N} \cdot \text{s}^8 \cdot \text{m}^{-1}$, $b_1 = 9.2806 \times 10^{-7} \text{ N} \cdot \text{s}^7 \cdot \text{m}^{-1}$, $b_2 = 1.6473 \times 10^{-4} \text{ N} \cdot \text{s}^6 \cdot \text{m}^{-1}$,
 548 $b_3 = 0.0024 \text{ N} \cdot \text{s}^5 \cdot \text{m}^{-1}$, $b_4 = 0.2132 \text{ N} \cdot \text{s}^4 \cdot \text{m}^{-1}$, $b_5 = 1.9781 \text{ N} \cdot \text{s}^3 \cdot \text{m}^{-1}$, $b_6 = 114.5197$
 549 $\text{N} \cdot \text{s}^2 \cdot \text{m}^{-1}$, $b_7 = 496.7671 \text{ N} \cdot \text{s} \cdot \text{m}^{-1}$ and $b_8 = 2.1588 \times 10^4 \text{ N} \cdot \text{m}^{-1}$.

550 References

551

552 [1] B.R. Ellis, T. Ji, Human-structure interaction in vertical vibrations, Proceedings of the
 553 Institution of Civil Engineers - Structures and Buildings, 122 (1997) 1-9.

554 [2] R. Sachse, The influences of human occupants on the dynamic properties of slender
 555 structures, PhD Thesis, University of Sheffield, 2003.

556 [3] R. Sachse, A. Pavic, P. Reynolds, Human-structure dynamic interaction in civil
 557 engineering dynamics: A literature review, Shock and Vibration Digest, 35 (2003) 3-18.

558 [4] E. Shahabpoor, A. Pavic, V. Racic, Interaction between walking humans and structures in
 559 vertical direction: a literature review, Shock and Vibration, 2016 (2016) 22.

560 [5] K. Van Nimmen, G. Lombaert, G. De Roeck, P. Van den Broeck, Reduced-order models
 561 for vertical human-structure interaction, Journal of Physics: Conference Series, 744 (2016)
 562 012030.

563 [6] X. Zheng, J.M.W. Brownjohn, Modeling and simulation of human-floor system under
 564 vertical vibration, in: L.P. Davis (Ed.) Proc. SPIE 4327, Smart Structures and Materials 2001:
 565 Smart Structures and Integrated Systems, Newport Beach, CA, USA, 2001, pp. 513-520.

566 [7] K. Van Nimmen, G. Lombaert, G. De Roeck, P. Van den Broeck, The impact of vertical
 567 human-structure interaction on the response of footbridges to pedestrian excitation, Journal of
 568 Sound and Vibration, 402 (2017) 104-121.

569 [8] P. Reynolds, A. Pavic, Z. Ibrahim, Changes of modal properties of a stadium structure
 570 occupied by a crowd, in: Proceedings of the 22nd international modal analysis conference,
 571 2004, pp. 421-428.

- 572 [9] R. Sachse, A. Pavic, P. Reynolds, Parametric study of modal properties of damped two-
573 degree-of-freedom crowd–structure dynamic systems, *Journal of Sound and Vibration*, 274
574 (2004) 461-480.
- 575 [10] J. Sim, A. Blakeborough, M. Williams, Modelling effects of passive crowds on
576 grandstand vibration, *Proceedings of the Institution of Civil Engineers - Structures and*
577 *Buildings*, 159 (2006) 261-272.
- 578 [11] J.M.W. Brownjohn, Energy dissipation from vibrating floor slabs due to human-
579 structure interaction, *Shock and Vibration*, 8 (2001).
- 580 [12] S.H. Kim, K. Cho, M. Choi, M.S. Choi, J.Y. Lim, Development of human body model
581 for the dynamic analysis of footbridges under pedestrian induced excitation, *Steel Structures*,
582 8 (2008) 333-345.
- 583 [13] E. Shahabpoor, A. Pavic, V. Racic, Identification of mass–spring–damper model of
584 walking humans, *Structures*, 5 (2016) 233-246.
- 585 [14] K. Van Nimmen, K. Maes, S. Zivanovic, G. Lombaert, G. De Roeck, P. Van den Broeck,
586 Identification and modelling of vertical human-structure interaction, in: J. Caicedo, S. Pakzad
587 (Eds.) *Dynamics of Civil Structures, Volume 2: Proceedings of the 33rd IMAC, A*
588 *Conference and Exposition on Structural Dynamics, 2015*, Springer International Publishing,
589 Cham, 2015, pp. 319-330.
- 590 [15] C.C. Caprani, E. Ahmadi, Formulation of human–structure interaction system models for
591 vertical vibration, *Journal of Sound and Vibration*, 377 (2016) 346-367.
- 592 [16] M. Zhang, C.T. Georgakis, W. Qu, J. Chen, SMD model parameters of pedestrians for
593 vertical human-structure interaction, in: J. Caicedo, S. Pakzad (Eds.) *Dynamics of Civil*
594 *Structures, Volume 2: Proceedings of the 33rd IMAC, A Conference and Exposition on*
595 *Structural Dynamics, 2015*, Springer International Publishing, Cham, 2015, pp. 311-317.
- 596 [17] L. Wei, M.J. Griffin, Mathematical models for the apparent mass of the seated human
597 body exposed to vertical vibration, *Journal of Sound and Vibration*, 212 (1998) 855-874.
- 598 [18] Y. Matsumoto, M.J. Griffin, Mathematical models for the apparent masses of standing
599 subjects exposed to vertical whole-body vibration, *Journal of Sound and Vibration*, 260 (2003)
600 431-451.
- 601 [19] R.O. Foschi, G.A. Neumann, F. Yao, B. Folz, Floor vibration due to occupants and
602 reliability-based design guidelines, *Canadian Journal of Civil Engineering*, 22 (1995) 471-
603 479.
- 604 [20] C.A. Jones, P. Reynolds, A. Pavic, Vibration serviceability of stadia structures subjected
605 to dynamic crowd loads: A literature review, *Journal of Sound and Vibration*, 330 (2011)
606 1531-1566.
- 607 [21] Y. Matsumoto, M.J. Griffin, Dynamic response of the standing human body exposed to
608 vertical vibration: Influence of posture and vibration magnitude, *Journal of Sound and*
609 *Vibration*, 212 (1998) 85-107.

- 610 [22] J. Sim, Human-structure interaction in cantilever grandstands, PhD Thesis, The
611 University of Oxford 2006.
- 612 [23] A. Kyprianou, J.E. Mottershead, H. Ouyang, Assignment of natural frequencies by an
613 added mass and one or more springs, *Mechanical Systems and Signal Processing*, 18 (2004)
614 263-289.
- 615 [24] X. Wei, J.E. Mottershead, Y.M. Ram, Partial pole placement by feedback control with
616 inaccessible degrees of freedom, *Mechanical Systems and Signal Processing*, 70–71 (2016)
617 334-344.
- 618 [25] X. Wei, J.E. Mottershead, Block-decoupling vibration control using eigenstructure
619 assignment, *Mechanical Systems and Signal Processing*, 74 (2016) 11-28.
- 620 [26] X. Wei, J.E. Mottershead, Aeroelastic systems with softening nonlinearity, *AIAA*
621 *Journal*, 52 (2014) 1915-1927.
- 622 [27] IStructE/DTLR/DCMS, Dynamic performance requirements for permanent grandstands
623 subject to crowd action, recommendations for management, design and assessment, The
624 Institution of Structural Engineers (IStructE), London, 2008.
- 625 [28] A. Pavic, P. Reynolds, Experimental verification of novel 3DOF model for grandstand
626 crowdstructure dynamic interaction, in: 26th international modal analysis conference:
627 IMAC-XXVI, Orlando, Florida, 2008.
- 628 [29] C.A. Jones, A. Pavic, P. Reynolds, R.E. Harrison, Verification of equivalent mass–
629 spring–damper models for crowd–structure vibration response prediction, *Canadian Journal*
630 *of Civil Engineering*, 38 (2011) 1122-1135.
- 631 [30] K.A. Salyards, N.C. Noss, Experimental evaluation of the influence of human-structure
632 interaction for vibration serviceability, *Journal of Performance of Constructed Facilities*, 28
633 (2014) 458-465.
- 634 [31] G.H. Golub, C.F. Van Loan, *Matrix computations*, 3rd ed, Baltimore, MD: Johns
635 Hopkins, 1996.
- 636 [32] B. Sudret, *Uncertainty propagation and sensitivity analysis in mechanical models–*
637 *Contributions to structural reliability and stochastic spectral methods, Habilitationa diriger*
638 *des recherches, Université Blaise Pascal, Clermont-Ferrand, France, (2007).*
- 639 [33] ISO, ISO 5982:1981 Vibration and shock -- Mechanical driving point impedance of the
640 human body, International Organisation for Standardisation (ISO), Geneva, Switzerland, 1981.
- 641 [34] S. Zivanovic, X. Wei, J. Russell, J.T. Mottram, Vibration performance of two FRP
642 footbridge structures in the United Kingdom, in: *Footbridge 2017*, Berlin, Germany, 2017.
- 643 [35] M.H. Richardson, D.L. Formenti, Parameter estimation from frequency response
644 measurements using rational fraction polynomials, in: *the 1st International Modal Analysis*
645 *Conference*, Orlando, FL, 1982.

646 [36] D. Formenti, M.H. Richardson, Global frequency & damping estimates from frequency
647 response measurements, in: 4th International Modal Analysis Conference, Los Angeles, CA,
648 1986.

649 [37] M. Abe, J.O. Smith III, Design criteria for simple sinusoidal parameter estimation based
650 on quadratic interpolation of FFT magnitude peaks, in: Audio Engineering Society
651 Convention 117, Audio Engineering Society, 2004.

652 [38] Z. Friedman, J.B. Kosmatka, An improved two-node Timoshenko beam finite element,
653 *Computers & Structures*, 47 (1993) 473-481.

654